CrossMark

ORIGINAL PAPER

Voltammetric determination of 17β-estradiol in human urine and buttermilk samples using a simple copper(II) oxide-modified carbon paste electrode

Cristiane Antoniazzi[1] · Camila Alves de Lima[1] · Rafael Marangoni[1] · Almir Spinelli[2] ·
Eryza Guimarães de Castro[1]

Abstract This paper reports the voltammetric determination of 17β-estradiol in urine and buttermilk samples using a simple detector based on a carbon paste electrode (CPE) modified with copper(II) oxide (CuO). The CuO was obtained by the Pechini method and characterized by X-ray diffraction (XRD), scanning electron microscopy (SEM), and energy-dispersive (EDS), Fourier transform infrared (FTIR), and Raman spectroscopies. Cyclic voltammetry (CV) and square-wave voltammetry (SWV) demonstrated that the CuO-modified carbon paste electrode (CuO/CPE detector) displayed much higher electrocatalytic activity in the 17β-estradiol oxidation reaction than the CPE without modification, exhibiting a low detection limit of 21.0 nmol L^{-1} with a wide linear range from 60.0 to 800.0 nmol L^{-1} ($R = 0.998$). Satisfactory results were obtained for the determination of 17β-estradiol in human urine and buttermilk samples. The proposed electrochemical detector offers high repeatability, stability, fast response, low cost, and potential for practical application in the quantification of this hormone.

Keywords 17β-Estradiol · Carbon paste electrode · CuO · Square-wave voltammetry

✉ Camila Alves de Lima
cami_delima@hotmail.com

1   Departamento de Química, Universidade Estadual do Centro-Oeste, Campus CEDETEG, Guarapuava, PR 85040-080, Brazil

2   Departamento de Química – CFM, Universidade Federal de Santa Catarina, Campus Reitor João David Ferreira Lima, Florianópolis, SC 88040-900, Brazil

Introduction

The three major naturally occurring forms of estrogen in women are estrone (E1), estradiol or 17β-estradiol (E2), and estriol (E3). E2 is the hormone responsible for the development and maintenance of the female reproductive system, and it also plays a role in the male reproduction system [1]. Furthermore, E2 is an endocrine-disrupting compound excreted by humans and domestic animals and it has high estrogenic activity. Endocrine-disrupting compounds can disturb the hormonal balance of an organism, and they have severe adverse effects on the health of humans and human fetuses, as well as on other animals, even in low concentration [2–4]. Researches have proved that low concentrations of E2 can cause the disequilibrium of humoral and cellular immunity, causing various pathological changes in the cardiovascular, immunological, reproductive, and nervous systems [5, 6]. Due to its use in hormonal contraceptives, hormone replacement therapy, and illegal animal growth promotion, the presence of E2 in the environment has been reported in recent years [7]. Thus, the development of simple, sensitive, reliable, and cost-effective methods for the determination of E2 levels in different types of samples has received considerable attention.

Methods previously described for the determination of E2 include gas chromatography [8], high-performance liquid chromatography [9], colorimetric [10], capillary electrophoresis [11], spectrophotometry-UV [12], and enzyme-linked immunosorbent assay [5]. Although these techniques are highly reliable and sensitive, the methods involve long analysis times, complex sample preparation procedures, and high costs. Electrochemical methods are useful alternatives with important advantages including fast response, low cost, ease of miniaturization, simplicity, reliability, and good sensitivity and selectivity [13–15].

Electrode modification is of great importance in electrochemistry as it enhances the sensitivity and selectivity toward a specific analyte in solution. The use of transition metal oxides as electrode modifiers has gained popularity in recent years due to their excellent electrocatalytic properties [16–18]. Among the numerous transition metal oxides, copper(II) oxide (CuO) is a promising material for electrode modification due to its high electrochemical activity, low cost, nontoxic characteristic, and easy preparation on the nanometric or microscopic scale [19, 20]. Recently, Beitollahi and coworkers [21] reported the use ZnO-CuO nanoplates to construct a modified carbon paste electrode (CPE) for the determination of 6-thioguanine in tablet and urine samples. The peak current of 6-thioguanine increased linearly in the concentration range of 50.0 to 200.000.0 nmol L^{-1}. The detection limit was 25.0 nmol L^{-1}. Furthermore, Soomro and coworkers [22] reported an electrochemical sensor based on a GCE modified with CuO nanostructures for the detection of malathion, an organophosphate pesticide. Under optimized conditions, the modified electrode showed a linear response for concentrations ranging from 1.0 to 12.0 nmol L^{-1} with a detection limit of 0.1 nmol L^{-1}. In another approach, Saleh and coworkers [23] fabricated a pencil graphite electrode modified with copper microparticles for the determination of the antiviral drug valacyclovir. The calibration curve was linear from 2.0 to 10.0 nmol L^{-1} with a detection limit of 0.178 nmol L^{-1}. The modified electrode was applied in the determination of valacyclovir in tablets. CuO shuttle-like nanocrystals on a polyneutral red glassy carbon electrode were constructed for the detection of guanine and adenine. Under optimized experimental conditions, the linear relationship between peak current and concentration was obtained in the range from 50.0 to 3000.0 nmol L^{-1} for guanine and adenine. A detection limit of 16.0 nmol L^{-1} was obtained for guanine and 23.0 nmol L^{-1} for adenine [24].

Moreover, the application of CuO as a component of electrochemical devices has been demonstrated in the detection of different compounds, such as hydrogen peroxide [25], glucose [26–32], DNA [33], and amino acids [34]. However, to the best of our knowledge, no studies on the development of electrochemical detectors for E2 using CuO have been previously reported.

Many approaches to preparing CuO have been described including thermal oxidation [35], hydrothermal [36], microwave [37], wet chemistry [38], electrodeposition [39], combustion [20], and controlled deposition [40] methods. Pechini's method [41] can also be applied in the synthesis of CuO. This procedure is advantageous because of its low cost, high yield, and simple operation, making it appropriate for large-scale synthesis.

In this context, the objective of this study was to describe the preparation and application of a simple, easy-to-prepare, and low-cost CuO-modified carbon paste electrode as a

detector for E2 with good sensitivity. The electrochemical behavior of E2 was investigated by cyclic and square-wave voltammetries at the proposed modified electrode. The influence of the CuO percentage in the CPE, scan rate, solution pH, chemical composition of the supporting electrolyte, and the square-wave voltammetry (SWV) parameters on the electrochemical oxidation of E2 was investigated in order to optimize the proposed modified electrode. The CuO/CPE obtained was successfully applied for the determination of E2 in urine and buttermilk samples.

Experimental

Reagents, solutions, and samples

All chemicals used in the experimental study were of analytical grade and obtained from Sigma-Aldrich. They were employed without any further purification. Two solutions were tested as the supporting electrolyte: 0.1 mol L^{-1} Britton-Robinson (B-R buffer) ($H_3BO_3/CH_3COOH/H_3PO_4$) and $H_3BO_3 \cdot KCl/NaOH$. The pH was adjusted with 0.5 mol L^{-1} HCl or NaOH solutions. All aqueous solutions were prepared with ultrapure water, produced in a TKA GenPure UV system (USA). All experiments were carried out at room temperature. A stock solution of 1.0 mmol L^{-1} E2 was prepared by dissolving the appropriate amount of the compound in ethanol. Less concentrated solutions were prepared by dilution. For the E2 determination and the recovery experiments, the standard addition method was used, with a standard solution of E2 being added to the samples. The urine sample was obtained from a healthy volunteer, and the buttermilk sample was acquired in the region of Laranjeiras do Sul, Paraná, Brazil.

Synthesis of the CuO

CuO was synthesized by the Pechini method: citric acid (0.78 g) was dissolved in deionized water (20 mL) under magnetic stirring at 90 °C until complete homogenization (solution 1). Copper(II) nitrate (1.55 g) and ethylene glycol (1.07 mL) were added to solution 1 and continuously stirred for 3 h at 90 °C to form a blue-colored gel. Lastly, the gel was calcined in a muffle furnace at 700 °C for 1 h. The resulting CuO solid was macerated in an agate mortar with a pestle.

Apparatus

XRD analysis was performed on a Bruker D2 Phaser diffractometer equipped with a LynxEye detector and copper ($\lambda K\alpha = 1.54$ Å) radiation source. FTIR spectra were collected on a Nicolet FTIR spectrophotometer, model FTIR-200, using KBr pellets. Raman spectra were registered using a WITec

300R Alpha confocal Raman microscope equipped with 523 nm laser excitation and a ×20 objective. Raman spectra were obtained at the Institute of Chemistry of the University of São Paulo, SP, Brazil.

The surface morphologies were evaluated by SEM and EDS using a TESCAN electron microscope (model VEGA3 LMU) with a secondary electron detector.

Cyclic voltammetry (CV) and SWV were performed using a potentiostat/galvanostat, model μ-autolab Type III (Metrohm, The Netherlands) interfaced to a personal computer with Nova software (version 1.10) for the acquisition and processing of data. The electrode system consisted of the CPE (unmodified or modified) as the working electrode, an Ag/AgCl (saturated KCl) as reference electrode, and a Pt wire as auxiliary electrode. A conventional glass cell encompassed the three electrodes and the solutions used for the experiments.

Preparation of the CuO/CPE detector

The unmodified CPE used for comparison was prepared by hand mixing of 75% graphite powder and 25% Nujol oil. The mixture was ground thoroughly in an agate mortar with a pestle for 20 min, and a homogeneous paste was obtained. The CuO/CPE detector was prepared by mixing CuO with graphite and a suitable amount of Nujol oil. The amount of CuO was varied from 10 to 40%, and the best results were obtained with 25% of CuO in the paste. Both unmodified and

modified pastes were placed firmly into a plastic syringe with a copper wire as the conductor. To ensure an active and fresh surface, the CuO/CPE detector was manually abraded gently on a sheet of paper between experiments.

Results and discussion

Characterization of the as-prepared CuO

The XRD pattern for CuO can be observed in Fig. 1a. The characteristic peaks of CuO at $2\theta = 35.46°$, $38.70°$, and $48.78°$ correspond to the Miller indices (-111), (111), and (-202), respectively (PDF No. 01-073-6023). The CuO phase is monoclinic; the space group $C2/c$ and the lattice constants are $a = 4.683$ Å, $b = 3.422$ Å, and $c = 5.128$ Å, which are consistent with data previously published in the literature [40]. The FTIR spectrum for the synthesized CuO is shown in Fig. 1b. The bands at 418, 458, 485, 518, 578, and 668 cm^{-1} are attributed to the framework vibration of the metal oxide (Cu-O stretching) [42]. Figure 1c shows the Raman spectrum for the CuO, which is characterized by bands at 292, 338, and 620 cm^{-1}, corresponding to the A_g and B_g modes of CuO, respectively [43]. The bands at 133 and 216 cm^{-1} suggest the presence of a small amount of Cu$_2$O [44].

The morphology of the CuO distribution was examined by SEM (Fig. 2). The micrograph reveals uniformity in the

Fig. 1 **a** XRD pattern, **b** FTIR spectrum, and **c** Raman spectrum of the as-prepared CuO
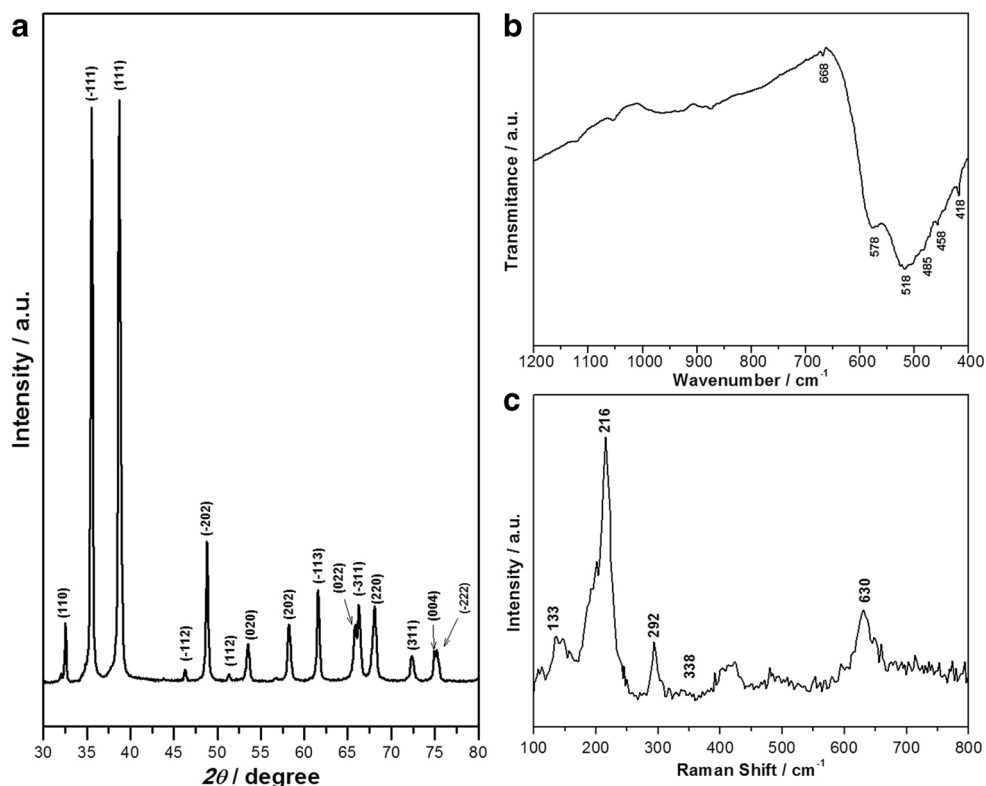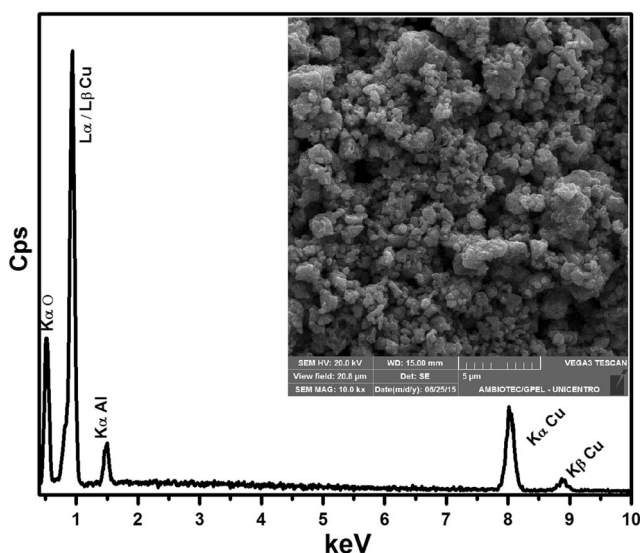
Fig. 2 EDS spectrum and SEM images of the as-prepared CuO

particle size distribution and shape and a flake-like morphology, in agreement with data obtained by other authors [45]. The chemical composition of the CuO obtained was determined using EDS, which showed the presence of copper, oxygen, and aluminum (from the SEM grid). This set of analyses demonstrated that the synthesis of CuO was successfully carried out.

Electrochemical response to E2 at the CuO/CPE detector determined by cyclic voltammetry

The electrochemical oxidation of 33.33 μmol L^{-1} E2 in 0.1 mol L^{-1} B-R buffer (pH 8.0) was studied by CV using the bare CPE and CuO/CPE detectors (Fig. 3). Cyclic voltammograms were obtained in the potential window range of 0.0 to +0.8 V with a scan rate (v) of 100 mV s^{-1}. As expected, no peaks were observed in the absence of E2 for the CuO/CPE detector (curve a). In contrast, in the presence of 33.33 μmol L^{-1} E2, an oxidation peak appeared at +0.581 V
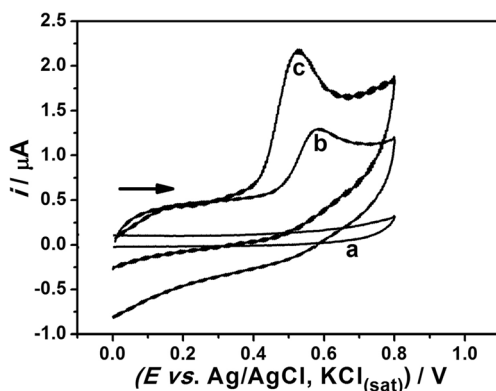

Fig. 3 Cyclic voltammograms in a 0.1 mol L^{-1} B-R buffer (pH 8.0) and in the presence of b, c 33.33 μmol L^{-1} E2 at the a, c CuO/CPE detector and b bare CPE, $v = 100$ mV s^{-1}

with a current of 0.427 μA for the CPE (curve b), while for the CuO/CPE detector (curve c), an oxidation peak appeared at a less positive potential (+0.523 V) and the current was 1.13 μA. These data clearly demonstrate that CuO increased the catalytic activity of the CPE regarding E2 oxidation. Such behavior could be explained taking into consideration some theoretical aspects of thermodynamic and kinetic electrochemistry, as follows: the diffusion of E2 to the electrode surface and of the oxidation product from the electrode surface can be the reaction rate-determining step, as predicted in heterogeneous catalysis. Kinetically, the reaction rate-determining step depends on the number of contacts of reagents (E2) with the electrode surface. Hence, it is conceivable that the presence of CuO at the CPE increased the surface area, which allowed the increase of frequency of contact of E2 molecules with the electrode surface promoted by an increase of E2 diffusion to the proposed detector, increasing the anodic current and shifting the oxidation potential to less negative values.

Effect of the CuO percentage

The content of CuO in the CPE significantly affects the performance of the CuO/CPE detector. To optimize the detector performance in order to obtain the best response for E2 oxidation, the effect of the CuO percentage on the current response was evaluated for percentages of 10 to 40% (w/w) (Fig. 4). It was observed that the current obtained by CV for the oxidation of 33.33 μmol L^{-1} E2 in 0.1 mol L^{-1} B-R buffer (pH 8.0) at the CuO/CPE detector reached the maximum value with 25% CuO in the paste, with a good voltammetric peak resolution. Above this value, the response was poor and the reproducibility of the voltammograms obtained was low. Thus, the percentage of CuO chosen for the construction of the CuO/CPE detector was 25%.

Effect of pH and chemical composition of the supporting electrolyte

Figure 5a shows the cyclic voltammograms for 66.66 μmol L^{-1} E2 in 0.1 mol L^{-1} B-R buffer at different pH values using the CuO/CPE detector. It can be observed that the E2 was electrochemically active at the proposed detector at pH 8.0 to 12.0. The anodic peak current—i_{pa}, as shown in Fig. 5b, increased from pH 8.0 to pH 9.0 and then decreased up to pH 12.0. It can be clearly observed that the highest anodic current was obtained at pH 9.0, which was chosen as the optimum pH for subsequent experiments. Figure 5c shows that the solution pH has a significant influence on the oxidation peak potential—E_{po}—of E2. It is clearly seen that E_{po} shifted to less positive potentials with an increase in the solution pH. The analysis of the dependence of E_{po} on the solution pH provided information on the E2
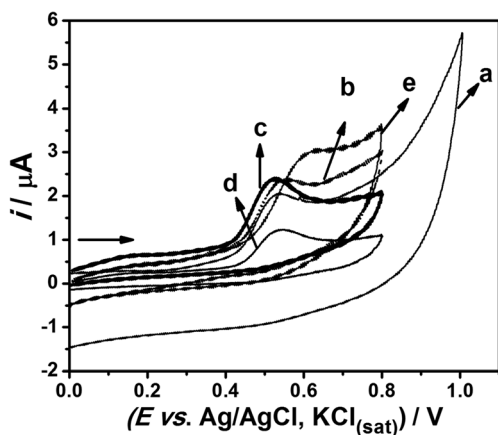
Fig. 4 Cyclic voltammograms for 33.33 μmol L^{-1} E2 in 0.1 mol L^{-1} B-R buffer (pH 8.0) using the CuO/CPE detector with the following percentages of CuO in the paste: *a* 10%, *b* 20%, *c* 25%, *d* 30%, and *e* 40%, *v* = 100 mV s^{-1}

electrooxidation mechanism. The linear regression equation can be expressed as $E_{po}/V = (1.01 \pm 0.02) - (0.061 \pm 0.002)$ pH. The slope of the straight line obtained was -61 mV pH^{-1}. According to the Nernst equation, for pH-dependent reversible reactions, the slope of $E_p \times$ pH plot is -59 mV pH^{-1}, when an equal number of protons and electrons is involved in the oxidation reaction. Although the electrochemical oxidation reaction of E2 is irreversible, as shown above, the slope of the graph $E_{po} \times$ pH suggests that the reaction path may be like that of a reversible reaction. This finding has previously been also reported by other authors [46, 47].

In the next step, the influence of different supporting electrolytes at pH 9.0 on the electrochemical response to E2 was evaluated (Fig. 6). The buffer solutions tested were H$_3$BO$_3$· KCl/NaOH (curve a) and B-R buffer (curve b). As demonstrated, the highest peak current was obtained in B-R buffer. Therefore, this buffered solution was chosen for further experiments.

Effect of scan rate

The effect of v on the E2 oxidation at the CuO/CPE detector was investigated by CV in B-R buffer (pH 9.0) (Fig. 7). The corresponding voltammograms are shown in Fig. 7a, where it can be seen that the E_{po} shifted slightly toward more positive values with an increase in v in the range of 20 to 250 mV s^{-1}. There is a linear relation between E_{po} and ln v according to the equation $E_{po}/V = (0.247 \pm 0.013) + (0.048 \pm 0.003)$ ln v, as shown in Fig. 7b. Based on the slope of this plot (0.048), it was possible to determine the number of electrons (n) involved in the oxidation of E2 at the proposed modified electrode. According to the Laviron theory [48], $2.303RT/(\alpha nF) =$ slope of plot E_{po} versus ln v for a totally irreversible electrode reaction process, where R is the universal gas

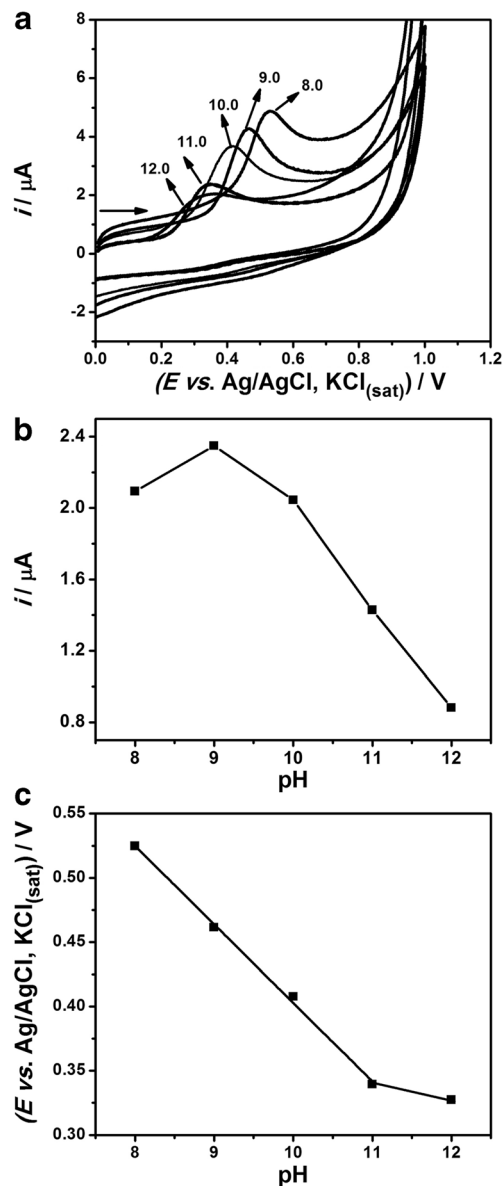**Fig. 5** **a** Cyclic voltammograms for 66.66 μmol L^{-1} E2 in 0.1 mol L^{-1} B-R buffer at the CuO/CPE detector, v = 100 mV s^{-1}. Influence of the supporting electrolyte pH on **b** i_{pa} and **c** E_{po}
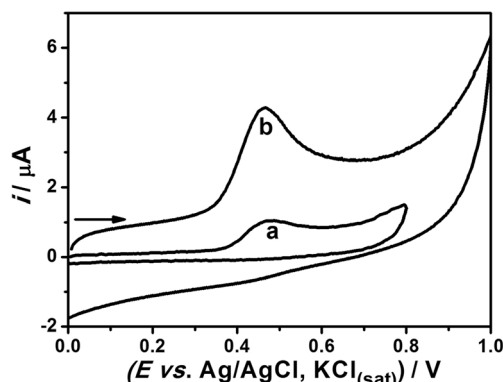

Fig. 6 Cyclic voltammograms for 66.66 μmol L^{-1} E2 in *a* H$_3$BO$_3$·KCl/ NaOH and *b* B-R buffers at pH 9.0 using the CuO/CPE detector, v = 100 mV s^{-1}
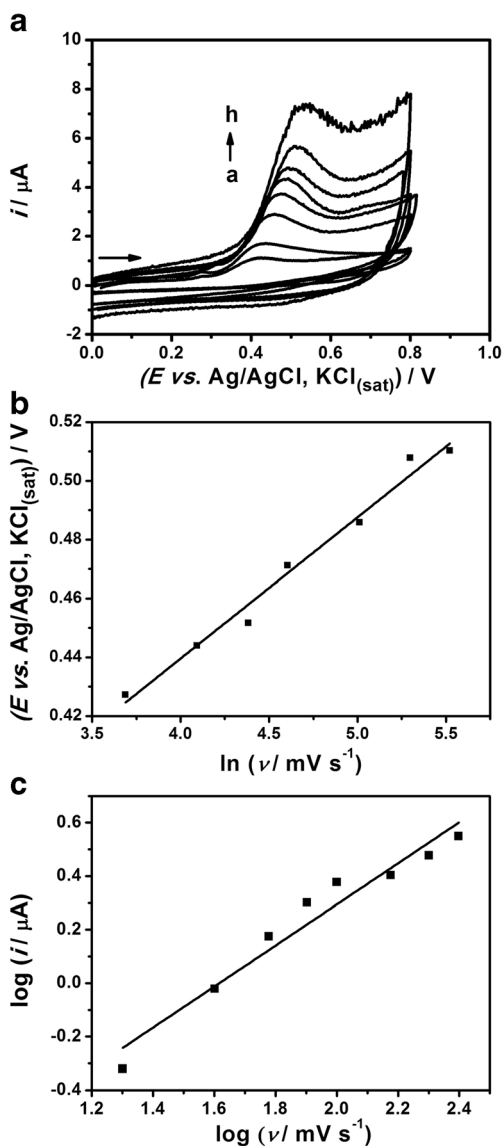
Fig. 7 **a** Cyclic voltammograms for 66.66 μmol L^{-1} E2 in 0.1 mol L^{-1} B-R buffer (pH 9.0) at the CuO/CPE detector, $v = a$ 20 mV s^{-1}, b 40 mV s^{-1}, c 60 mV s^{-1}, d 80 mV s^{-1}, e 100 mV s^{-1}, f 150 mV s^{-1}, g 200 mV s^{-1}, and h 250 mV s^{-1}. The relationship between **b** E_{po} and ln v, and between **c** log i_{pa} and log v

constant (8.314 J mol^{-1} K^{-1}), T is the temperature (298 K), α is the transfer coefficient, n is the number of electrons transferred, and F is the Faraday constant (96.480 C mol^{-1}). In agreement with reference [49], $\alpha = 0.5$ can be assumed for many reactions. Hence, the number of electrons calculated was around 1.0, signifying that one electron is involved in the E2 oxidation mechanism. For the same reaction, $n = 1$ has also been reported by other authors [15, 50]. In parallel, i_{pa} increased with an increase in v according to the equation: log i_{pa}/μA $= -(1.24 \pm 0.14) + (0.77 \pm 0.07)$ log v (Fig. 7c). The slope of 0.768 signifies that the E2 oxidation reaction on the CuO/CPE detector is controlled by a mixture of diffusion and adsorption.

Moraes and coworkers [15] propose that the electrochemical oxidation of E2 is an irreversible process in which one proton and one electron participate, giving the corresponding ketone derivative as product. According with our findings discussed above, the electrochemical oxidation of E2 at the CuO/CPE detector seems to follow the same mechanism pathway.

Electrochemical detection of E2 by square-wave voltammetry

Square-wave voltammograms were recorded at between 0.0 and +0.8 V for E2 in 0.1 mol L^{-1} B-R buffer (pH 9.0) at the CuO/CPE detector. Firstly, the square-wave parameters (frequency, amplitude, and scan increment) were optimized for E2 oxidation. The ranges studied were 10.0 to 100.0 Hz for frequency (f), 10.0 to 100.0 mV for amplitude (a), and 1.0 to 10.0 mV for scan increment (ΔEs). The values selected were 50.0 Hz, 50.0 mV, and 1.0 mV for frequency, amplitude, and scan increment, respectively, because they provided the best compromise between the voltammetric profile and sensitivity.

Under the optimized conditions previously established, the influence of the E2 concentration on the SWV curves was studied using the proposed CuO/CPE detector. The results obtained are shown in Fig. 8a. Based on the calibration curve shown in Fig. 8b, the linear range was between 60.0 and 800.0 nmol L^{-1}, and the corresponding regression equation is i_{pa}/μA $= (3.41 \pm 0.05)$[estradiol] $- (0.04 \pm 0.02)$ ($R = 0.998$). The limit of detection (LOD) and limit of quantification (LOQ) were calculated from the calibration curve as follows: LOD $= 3.3$(SD/b) and LOQ $= 10$(SD/b), where SD is the standard deviation of the y-coordinate obtained from the line of best fit (linear coefficient), and b is the slope (angular coefficient) of this straight line. The calculated LOD and LOQ values were 21.0 and 64.0 nmol L^{-1}, respectively. Other figures of merit obtained using the CuO/CPE for E2 detection are shown in Table 1.

For comparison purposes, calibration curves were constructed using a GCE (Fig. 9a) and a gold electrode (Fig. 9b), under the same conditions used to obtain Fig. 8. The linear regression equation obtained using the GCE was as follows: i_{pa}/μA $= (1.90 \pm 0.08)$ [estradiol] $- (0.22 \pm 0.05)$ ($R = 0.983$). The linear regression equation obtained using the gold electrode was as follows: i_{pa}/μA $= (1.35 \pm 0.06)$ [estradiol] $- (0.14 \pm 0.04)$ ($R = 0.979$). The LOD and LOQ values obtained with the GCE were 87.7 and 266.0 nmol L^{-1}, respectively, and for the gold electrode, the corresponding values were LOD $= 97.9$ nmol L^{-1} and LOQ $= 296.7$ nmol L^{-1}. These results indicate that the CuO/CPE is more sensitive than the bare GCE and gold in relation to E2 determination.

Table 2 compares the performance of the proposed modified CPE with that of several electrochemical devices reported in the literature for E2 determination. It can be observed that
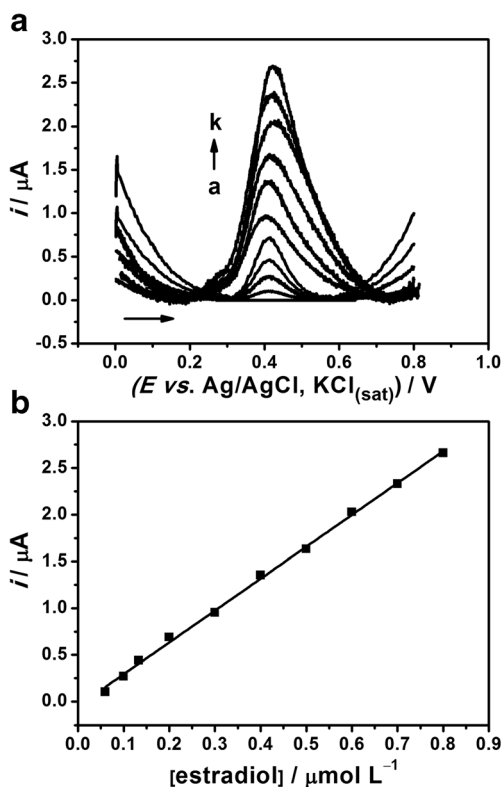
Fig. 8 **a** Square-wave voltammograms for *a* blank, *b* 0.06 µmol L⁻¹, *c* 0.10 µmol L⁻¹, *d* 0.13 µmol L⁻¹, *e* 0.2 µmol L⁻¹, *f* 0.3 µmol L⁻¹, *g* 0.4 µmol L⁻¹, *h* 0.5 µmol L⁻¹, *i* 0.6 µmol L⁻¹, *j* 0.7 µmol L⁻¹, and *k* 0.8 µmol L⁻¹ E2 in 0.1 mol L⁻¹ B-R buffer (pH 9.0) at the CuO/CPE detector. **b** The calibration curve. SWV parameters: f = 50.0 Hz, a = 50.0 mV, ΔEs = 1.0 mV

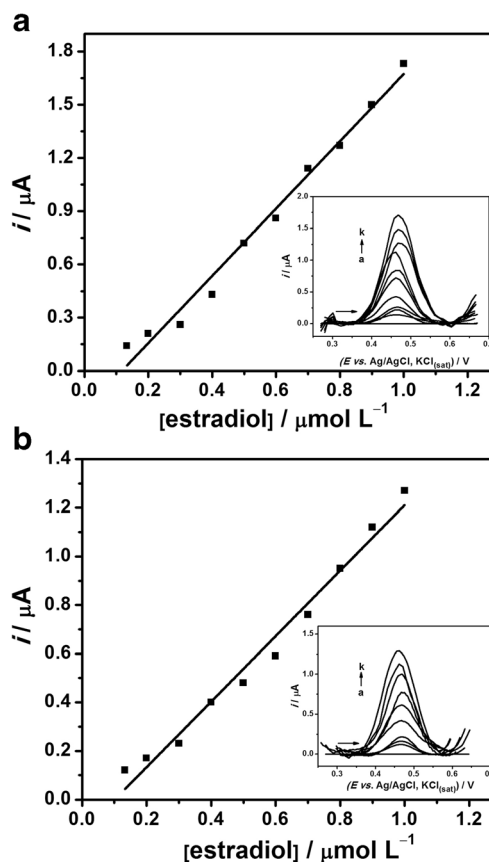**Fig. 9** Calibration curves for E2 using **a** GCE and **b** gold electrode. Square-wave voltammograms for *a* blank, *b* 0.13 µmol L⁻¹, *c* 0.2 µmol L⁻¹, *d* 0.3 µmol L⁻¹, *e* 0.4 µmol L⁻¹, *f* 0.5 µmol L⁻¹, *g* 0.6 µmol L⁻¹, *h* 0.7 µmol L⁻¹, *i* 0.8 µmol L⁻¹, *j* 0.9 µmol L⁻¹, and *k* 1.0 µmol L⁻¹ E2. SWV parameters: f = 50.0 Hz, a = 50.0 mV, ΔEs = 1.0 mV

the analytical characteristics of the CuO/CPE detector are better than or comparable with those of the other devices. Several detectors listed in Table 2 are electrodes modified with nanoparticulate materials or complex biosensors associated with laborious and expensive preparation procedures. On the other hand, the modified electrode proposed in this paper makes use of CuO microparticles, it is able to detect E2 at

the nanomolar level, and it is prepared through a simple procedure at low cost.

Repeatability, stability, and interference studies with the CuO/CPE detector

The repeatability of the current measured for the 0.1-µmol-L⁻¹ E2 oxidation at the CuO/CPE detector was estimated in 0.1 mol L⁻¹ B-R buffer (pH 9.0) by SWV. It was verified that the intra- and interday repeatability of the data obtained using the proposed electrochemical device was excellent. The relative standard deviation (RSD) of successive measurements on the same day (intraday repeatability) was 2.73% (n = 10). The interday repeatability was evaluated on 10 consecutive days using the same parameters and an RSD of 6.73% was obtained. The low values for the RSD indicate the high degree of precision of the data obtained when the CuO/CPE is used for E2 detection. To evaluate the stability of the as-prepared voltammetric device, the modified electrode was stored in air for 90 days. The peak current delivered after this time was 93.5% of its initial value. Therefore, the detector

Table 1 Analytical parameters obtained from the calibration curve for E2 using the CuO/CPE detector

Analytical parameter	Value
Peak potential (V)	+0.450
Linear range (nmol L⁻¹)	60.0 to 800.0
Correlation coefficient (R)	0.998
Slope (µA L mol⁻¹)	3.409
Standard deviation of slope (µA L mol⁻¹)	0.048
Intercept (µA)	0.045
Standard deviation of intercept (µA)	0.022
Limit of detection (nmol L⁻¹)	21.0
Limit of quantification (nmol L⁻¹)	64.0

Table 2 Performance of different sensors for E2 detection

Detector	Technique	Linear range (nmol L^{-1})	LOD (nmol L^{-1})	Reference
RGO–DHP/GCE	CV	400.0–20,000.0	77.0	[51]
BPIDS/GCE	DPV	100.0–10,000.0	50.0	[50]
Poly(L-serine)/GCE	LSV	100.0–30,000.0	20.0	[52]
PtNPs/GCE	CV	30.0–50,000.0	16.0	[53]
Pt/MWNTs/GCE	SWV	500.0–15,000.0	180.0	[54]
CNT/Ni/GCE	SWV	500.0–40,000.0	60.0	[55]
CuO/CPE detector	SWV	60.0–800.0	21.0	This study

RGO reduced graphene oxide, *DHP* dihexadecylphosphate, *GCE* glassy carbon electrode, *BPIDS* 1-butyl-3-[3-(*N*-pyrrole)propyl]imidazolium tetrafluoroborate, *PtNPs* platinum nanoparticles, *Pt* Pt nanoclusters, *MWNTs* multiwalled carbon nanotubes, *CNT* carbon nanotube, *Ni* Ni complex, *DPV* differential pulse voltammetry, *LSV* linear sweep voltammetry

developed in this study is stable and suitable for the routine analysis of E2 in different types of samples. An important parameter for new detectors is their ability to discriminate the interfering species commonly present in samples from the target analyte. In order to evaluate the selectivity of the CuO/CPE toward E2 in the presence of other chemical species, the influence of potentially interfering substances on the E2 anodic current was investigated. The potential interferents considered were glucose, sucrose, uric acid, urea, ascorbic acid, K$^+$, Na$^+$, Cl$^-$, and Ca^{2+}. The interferent/E2 ratios tested were 100/1, 1/1, and 1/100. The currents obtained by SWV for E2 oxidation were between 2.07 and 4.33% lower in the presence of interferents (data not shown). This behavior verifies that the CuO/CPE detector is suitable for the analyses of E2 in complex matrices, such as urine and buttermilk, because it is not significantly affected by the presence of potentially interfering species commonly present along with the molecule of interest.

Fig. 10 Square-wave voltammograms for **a** 50 μL of urine and **b** 200 μL of buttermilk: *a* blank, *b* samples, and *c–f* additions of 100, 200, 300, and 400 μL of 10.0 μmol L^{-1} E2. **c, d** The corresponding standard addition plots. Experimental conditions: CuO/CPE detector, 0.1 mol L^{-1} B-R buffer (pH 9.0), f = 50.0 Hz, a = 50.0 mV, ΔE_S = 1.0 mV
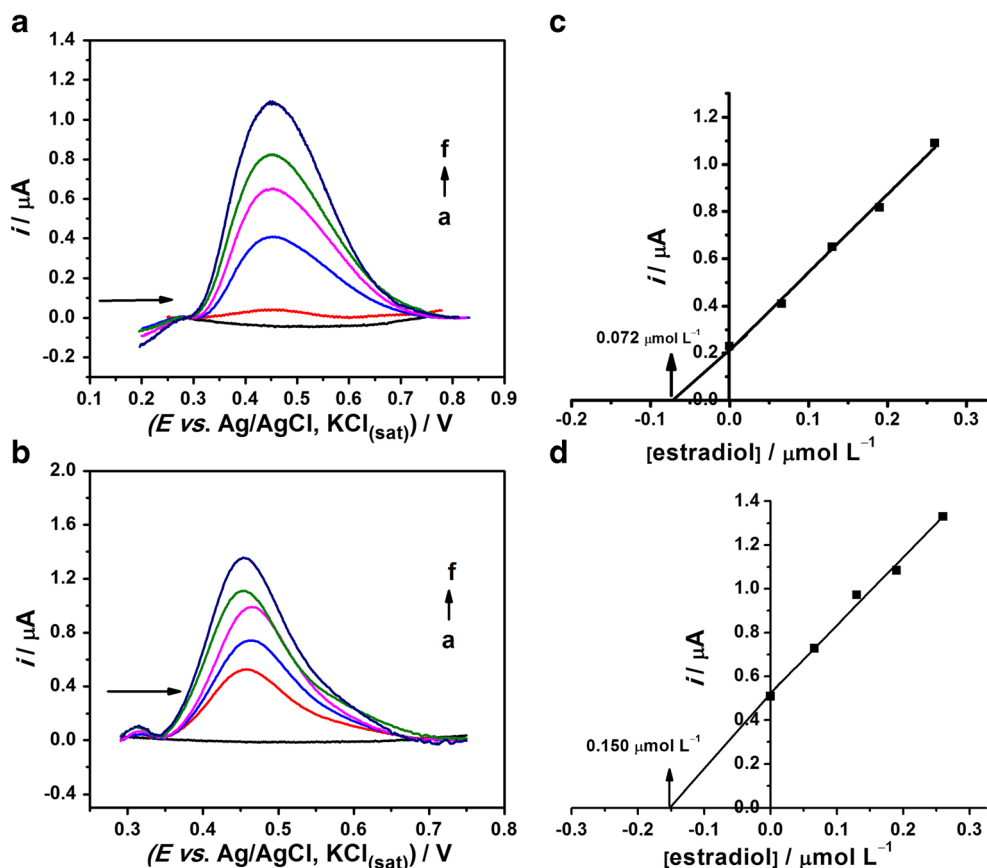
Table 3 Results for determination of E2 and recovery experiments with the samples analyzed

Sample	Determined[a] (nmol L^{-1})	Added (nmol L^{-1})	Found (nmol L^{-1})	Recovery (%)
Urine	72.0	130.0	200.0	99
		190.0	250.0	94
		260.0	350.0	107
Buttermilk	150.0	130.0	270.0	92
		190.0	360.0	110
		260.0	420.0	104

[a] Mean of three measurements taken under the same conditions

E2 determination in urine and buttermilk samples

The SWV results obtained in the determination of E2 in urine and buttermilk samples are shown in panels a and b of Fig. 10, respectively. The linear regressions obtained for the corresponding standard addition plots shown in Fig. 10c, d are as follows: urine ($y = (3.31 \pm 0.12)$ [estradiol] $+ (0.21 \pm 0.02)$) and buttermilk ($y = (3.10 \pm 0.16)$ [estradiol] $+ (0.52 \pm 0.02)$), where y is the current (μA) and [estradiol] is the E2 concentration (μmol L^{-1}). It can be observed, for both samples, that the slopes of the standard addition plot and the calibration curve (3.41 μA L mol^{-1}, Table 1) are very similar. This corroborates the results discussed above and confirms that the matrix components did not affect the determination of E2. In addition, these results demonstrate that the E2 concentration can be determined with high sensitivity and selectivity using the CuO/CPE detector.

The accuracy provided by the CuO/CPE detector for the determination of E2 was evaluated from recovery experiments. In brief, known amounts of standard E2 solution were added to the real samples followed by analysis using the standard addition method. The results obtained are given in Table 3. The recovery values for the two types of samples ranged from 92 to 107%. These results indicated that the fabricated modified electrode can be used as an electrochemical detector for E2 determination, since it provides accurate values.

Conclusions

In this study, CuO microparticles were successfully synthesized by Pechini's method using low-cost precursors and characterized using XRD, FTIR, Raman spectroscopy, SEM, and EDS. The XRD results indicate that the particles are monoclinic (crystalline). The Raman spectra exhibit three different bands, which correspond to the A_g and B_g modes of CuO. It was also observed that the morphology of the microparticles is flake-like with uniformity in the distributions of size and shape.

A simple CPE was modified with CuO microparticles and used for the detection of E2. The electrochemical behavior of E2 at the CuO/CPE detector was studied by CV, and it was found that the modified electrode led to enhanced sensitivity in the voltammetric detection of this hormone. This detector offers many beneficial analytical characteristics, such as a good detection limit of 21.0 nmol L^{-1}, wide linear concentration range of 60.0 to 800.0 nmol L^{-1}, and a good repeatability, stability, and selectivity. The proposed detector was successfully applied to the analysis of urine and buttermilk samples with satisfactory recovery values (92–110%).

The proposed CuO/CPE detector offers certain advantages over conventional electrodes including ease of fabrication, high electrochemical activity, simplicity, and low cost, and in association with SWV, it provided low limits of detection and quantification. Based on the results obtained, the CuO/CPE showed satisfactory performance in comparison with other electrodes used for the determination of E2. It can thus be concluded that the use of the proposed CuO/CPE detector represents a promising technique for the determination of E2 in real and complex samples, without the need for elaborate sample preparation procedures. The improvement achieved can be attributed to the combination of graphite powder and CuO and the resulting synergistic effect. The results reported herein demonstrate that CuO microparticles can offer better potential for application in comparison with nanoparticles of transition metal oxides.

References

1. Li Y, Zhao X, Li P, Huang Y, Wang J, Zhang J (2015) Highly sensitive Fe$_3$O$_4$ nanobeads/graphene-based molecularly imprinted electrochemical sensor for 17β-estradiol in water. Anal Chim Acta 884:106–113

2. Omar TFT, Ahmad A, Aris AZ, Yusoff FM (2016) Endocrine disrupting compounds (EDCs) in environmental matrices: review of analytical strategies for pharmaceuticals, estrogenic hormones, and alkylphenol compounds. TrAC Trends Anal Chem 85:241–259

3. Liu H, Yang X, Lu R (2016) Development of classification model and QSAR model for predicting binding affinity of endocrine disrupting chemicals to human sex hormone-binding globulin. Chemosphere 156:1–7

4. Scsukova S, Rollerova E, Bujnakova AM (2016) Impact of endocrine disrupting chemicals on onset and development of female reproductive disorders and hormone-related cancer. Biol Reprod 16:243–254

5. Silva CP, Lima DLD, Schneider RJ, Otero M, Esteves VI (2013) Development of ELISA methodologies for the direct determination of 17β-estradiol and 17α-ethinylestradiol in complex aqueous matrices. J Environ Manag 124:121–127

6. Hu L, Cheng Q, Chen D, Ma M, Wu K (2015) Liquid-phase exfoliated graphene as highly-sensitive sensor for simultaneous determination of endocrine disruptors: diethylstilbestrol and estradiol. J Hazard Mater 283:157–163

7. Tseng TTC, Gusviputri A, Hoa LNQ (2015) A simple, sensitive and compact electrochemical ELISA for estradiol based on chitosan deposited platinum wire microelectrodes. J Electroanal Chem 758:59–67

8. Feng H, Ning L, Xiao-Li L (2016) Simultaneous determination of hexoestrol, diethylstilbestrol, estrone and 17-beta-estradiol in feed by gas chromatography-mass spectrometry. J Northeast Agric Univ 23:44–49

9. Shahbazi Y, Malekinejad H, Tajik H (2016) Determination of naturally occurring estrogenic hormones in cow's and river buffalo's meat by HPLC-FLD method. J Food Drug Anal 24:457–463

10. Li Y, Xu J, Jia M, Yang Z, Liang Z, Guo J, Luo Y, Shen F, Sun C (2015) Colorimetric determination of 17β-estradiol based on the specific recognition of aptamer and the salt-induced aggregation of gold nanoparticles. Mater Lett 159:221–224

11. Regan F, Moran A, Fogarty B, Dempsey E (2003) Novel modes of capillary electrophoresis for the determination of endocrine disrupting chemicals. J Chromatogr A 1014:141–152

12. Yilmaz B, Kadioglu Y (2013) Determination of 17 β-estradiol in pharmaceutical preparation by UV spectrophotometry and high performance liquid chromatography methods. Arab J Chem 10:1422–1428

13. Cesarino I, Hümmelgen IA (2015) An additional tool towards overcoming absence of specificity of carbon nanostructure-based electrochemical sensors—application to estriol and estradiol detection and distinction. J Solid State Electrochem 19:3035–3050

14. Perez C, Fábio RS, Codognoto L (2015) Voltammetric determination of 17α-ethinylestradiol hormone in supply dam using BDD electrode. J Solid State Electrochem 20:2471–2478

15. Moraes FC, Rossi B, Donatoni MC, de Oliveira KT, Pereira EC (2015) Sensitive determination of 17β-estradiol in river water using a graphene based electrochemical sensor. Anal Chim Acta 881:37–43

16. Erogul S, Bas SZ, Ozmen M, Yildiz S (2015) A new electrochemical sensor based on Fe₃O₄ functionalized graphene oxide-gold nanoparticle composite film for simultaneous determination of catechol and hydroquinone. Electrochim Acta 186:302–313

17. Gao F, Zheng D, Tanaka H, Zhan F, Yuan X, Gao F, Wang Q (2015) An electrochemical sensor for gallic acid based on Fe₂O₃/electro-reduced graphene oxide composite: estimation for the antioxidant capacity index of wines. Mater Sci Eng C 57:279–287

18. Nguyen TT, Nguyen VH, Deivasigamani RK, Kharismadewi D, Iwai Y, Shim JJ (2016) Facile synthesis of cobalt oxide/reduced graphene oxide composites for electrochemical capacitor and sensor applications. Solid State Sci 53:71–77

19. Kim SH, Umar A, Kumar R, Ibrahim AA, Kumar G (2015) Facile synthesis and photocatalytic activity of cocoon-shaped CuO nanostructures. Mater Lett 156:138–141

20. Dong C, Xiao X, Chen G, Guan H, Wang Y (2015) Morphology control of porous CuO by surfactant using combustion method. Appl Surf Sci 349:844–848

21. Beitollahi H, Ivari SG, Torkzadeh-Mahani M (2016) Voltammetric determination of 6-thioguanine and folic acid using a carbon paste electrode modified with ZnO-CuO nanoplates and modifier. Mater Sci Eng C 69:128–133

22. Soomro RA, Hallam KR, Ibupoto ZH, Tahira A, Sherazi STH, Sirajjuddin SSM, Willander M (2016) Amino acid assisted growth of CuO nanostructures and their potential application in electrochemical sensing of organophosphate pesticide. Electrochim Acta 190:972–979

23. Saleh GA, Askal HF, Refaat IH, Naggar AH, Abdel-aal FAM (2016) Adsorptive square wave voltammetric determination of the antiviral drug valacyclovir on a novel sensor of copper microparticles–modified pencil graphite electrode. Arab J Chem 9:143–151

24. Liang X, Zhang X, Wang F, Xu M, Bao X (2014) Simultaneous determination of guanine and adenine on CuO shuttle-like nanocrystals/poly(neutral red) film on glassy carbon electrode. J Solid State Electrochem 18:3453–3461

25. Song H, Ni Y, Kokot S (2015) A novel electrochemical sensor based on the copper-doped copper oxide nano-particles for the analysis of hydrogen peroxide. Colloids Surf A Physicochem Eng Asp 465:153–158

26. Ghanbari K, Babaei Z (2016) Fabrication and characterization of non-enzymatic glucose sensor based on ternary NiO/CuO/polyaniline nanocomposite. Anal Biochem 498:37–46

27. Farid MM, Goudini L, Piri F, Zamani A, Saadati F (2016) Molecular imprinting method for fabricating novel glucose sensor: polyvinyl acetate electrode reinforced by MnO₂/CuO loaded on graphene oxide nanoparticles. Food Chem 194:61–67

28. Lu N, Shao C, Li X, Miao F, Wang K, Liu Y (2016) CuO nanoparticles/nitrogen-doped carbon nanofibers modified glassy carbon electrodes for non-enzymatic glucose sensors with improved sensitivity. Ceram Int 42:11285–11293

29. Liu XW, Pan P, Zhang ZM, Guo F, Yang ZC, Wei J, Wei Z (2016) Ordered self-assembly of screen-printed flower-like CuO and CuO/MWCNTs modified graphite electrodes and applications in non-enzymatic glucose sensor. J Electroanal Chem 763:37–44

30. Zhong Y, Shi T, Liu Z, Cheng S, Huang Y, Tao X, Liao G, Tang Z (2016) Ultrasensitive non-enzymatic glucose sensors based on different copper oxide nanostructures by in-situ growth. Sensors Actuators B Chem 236:326–333

31. Medeiros NG, Ribas VC, Lavayen V, Da Silva JA (2016) Synthesis of flower-like cuo hierarchical nanostructures as an electrochemical platform for glucose sensing. J Solid State Electrochem 20:2419–2426

32. Yang YJ, Li W, Chen X (2012) Highly enhanced electrocatalytic oxidation of glucose on Cu (OH)₂/CuO nanotube arrays modified copper electrode. J Solid State Electrochem 16:2877–2881

33. Chen M, Hou C, Huo D, Yang M, Fa H (2016) An ultrasensitive electrochemical DNA biosensor based on a copper oxide nanowires/single-walled carbon nanotubes nanocomposite. Appl Surf Sci 364:703–709

34. Gutierrez FA, Rubiane MD, Rivas GA (2016) Electrochemical sensor for amino acids and glucose based on glassy carbon electrodes modified with multi-walled carbon nanotubes and copper microparticles dispersed in polyethylenimine. J Electroanal Chem 765:16–21

35. Yurddaskal M, Dikici T, Celik E (2016) Effect of annealing temperature on the surface properties and photocatalytic efficiencies of Cu₂O/CuO structures obtained by thermal oxidation of Cu layer on titanium substrates. Ceram Int 42:17749–17753

36. Bhuvaneshwari S, Gopalakrishnan N (2016) Hydrothermally synthesized copper oxide (CuO) superstructures for ammonia sensing. J Colloid Interface Sci 480:76–84

37. Nahas MN, Jilani A, Salah N (2016) Microwave synthesis of ultra-thin, non-agglomerated CuO nanosheets and their evaluation as nanofillers for polymer nanocomposites. J Alloys Compd 680:350–358

38. Agarwal R, Verma K, Agrawal NK, Duchaniya RK, Singh R (2016) Synthesis, characterization, thermal conductivity and sensitivity of CuO nanofluids. Appl Therm Eng 102:1024–1036

39. Wang Y, Jiang T, Meng D, Yang J, Li Y, Ma Q, Han J (2014) Fabrication of nanostructured CuO films by electrodeposition and their photocatalytic properties. Appl Surf Sci 317:414–421

40. Lugo-Ruelas M, Amézaga-Madrid P, Esquivel-Pereyra O, Antúnez-Flores W, Pizá-Ruiz P, Ornelas-Gutiérrez C, Miki-Yoshida M (2015) Synthesis, microstructural characterization and optical properties of CuO nanorods and nanowires obtained by aerosol assisted CVD. J Alloys Compd 643:S46–S50

41. Alhaji A, Razavi RS, Ghasemi A, Loghman-Estarki MR (2017) Modification of Pechini sol–gel process for the synthesis of MgO-Y_2O_3 composite nanopowder using sucrose-mediated technique. Ceram Int 43:2541–2548

42. Jan T, Iqbal J, Farooq U, Gul A, Abbasi R, Ahmad I, Malik M (2015) Structural, Raman and optical characteristics of Sn doped CuO nanostructures: a novel anticancer agent. Ceram Int 41:13074–13079

43. Ganga BG, Santhosh PN (2015) Facile synthesis of porous copper oxide nanostructure using copper hydroxide acetate precursor. Mater Lett 138:113–115

44. Sahai A, Goswami N, Kaushik SD, Tripathi S (2016) Cu/Cu_2O/CuO nanoparticles: novel synthesis by exploding wire technique and extensive characterization. Appl Surf Sci 390:974–983

45. Ananth A, Dharaneedharan S, Heo MS, Mok YS (2015) Copper oxide nanomaterials: synthesis, characterization and structure-specific antibacterial performance. Chem Eng J 262:179–188

46. Hamid H, Eskicioglu C (2012) Fate of estrogenic hormones in wastewater and sludge treatment: a review of properties and analytical detection techniques in sludge matrix. Water Res 46:5813–5833

47. Lahcen AA, Baleg AA, Baker P, Iwuoha E, Amine A (2017) Synthesis and electrochemical characterization of nanostructured magnetic molecularly imprinted polymers for 17-β-estradiol determination. Sensors Actuators B Chem 241:698–705

48. Laviron E (1979) General expression of the linear potential sweep voltammogram in the case of diffusionless electrochemical systems. J Electroanal Chem 101:19–28

49. Bard AJ, Faulkner LR (2001) Electrochemical methods: fundamentals and applications. Wiley, New York

50. Wang T, Su W, Fu Y, Hu J (2016) Controllably annealed CuO-nanoparticle modified ITO electrodes: characterisation and electrochemical studies. Appl Surf Sci 390:795–803

51. Janegitz BC, dos Santos FA, Faria RC, Zucolotto V (2014) Electrochemical determination of estradiol using a thin film containing reduced graphene oxide and dihexadecylphosphate. Mater Sci Eng C 37:14–19

52. Song J, Yang J, Hu X (2008) Electrochemical determination of estradiol using a poly(l-serine) film-modified electrode. J Appl Electrochem 38:833–836

53. Yuan L, Zhang J, Zhou P, Chen J, Wang R, Wen T, Li Y, Zhou X, Jiang H (2011) Electrochemical sensor based on molecularly imprinted membranes at platinum nanoparticles-modified electrode for determination of 17β-estradiol. Biosens Bioelectron 29:29–33

54. Lin X, Li Y (2006) A sensitive determination of estrogens with a Pt nano-clusters/multi-walled carbon nanotubes modified glassy carbon electrode. Biosens Bioelectron 22:253–259

55. Liu X, Wong DKY (2007) Electrocatalytic detection of estradiol at a carbon nanotube Ni(Cyclam) composite electrode fabricated based on a two-factorial design. Anal Chim Acta 594:184–191